

1    **Aligning Climate and Health Co-benefits through Supply-  
2    Chain Energy Intensity Coordination in China**

3    Jiao Du<sup>1,2</sup>, Yilin Chen<sup>1,2\*</sup>, Huizhong Shen<sup>2</sup>, Jing Meng<sup>3</sup>, Jianmin Ma<sup>4</sup>, Guofeng Shen<sup>4</sup>,  
4    Armistead G. Russell<sup>5</sup>, Shunliu Zhao<sup>6</sup>, Amir Hakami<sup>6</sup>, Shu Tao<sup>2,4</sup>

5    <sup>1</sup>School of Urban Planning and Design, Peking University Shenzhen Graduate School,  
6    Shenzhen 518055, China.

7    <sup>2</sup>Shenzhen Key Laboratory of Precision Measurement and Early Warning Technology for Urban  
8    Environmental Health Risks, School of Environmental Science and Engineering, Southern  
9    University of Science and Technology, Shenzhen 518055, China.

10    <sup>3</sup>The Bartlett School of Sustainable Construction, University College London, London WC1E  
11    6BT, UK.

12    <sup>4</sup>College of Urban and Environmental Sciences, Peking University, Beijing 100871, China.

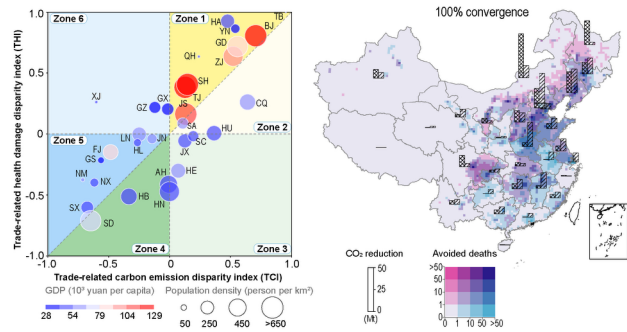
13    <sup>5</sup>School of Civil and Environmental Engineering, Georgia Institute of Technology, Atlanta, GA  
14    30332, USA.

15    <sup>6</sup>Department of Civil and Environmental Engineering, Carleton University, Ottawa, ON  
16    K1S5B6, Canada.

17    \*Corresponding author, e-mail: [ylchen2023@pku.edu.cn](mailto:ylchen2023@pku.edu.cn)

18

19    **Word Count: Approximately 6800 word-equivalents.**



22 **Abstract**

23 The co-mitigation of carbon emissions and air pollutants offers substantial benefits but is  
24 complicated by divergent sectoral emission profiles and spatial disparities. By integrating input-  
25 output analysis with health impact source attribution, we examine how interprovincial trade  
26 redistributes CO<sub>2</sub> emissions and PM<sub>2.5</sub>-related mortality across China's supply chains. We find  
27 that demand from economically advanced provinces induces two distinct burden-shifting  
28 patterns between carbon emissions and health burdens. Carbon emissions are outsourced to  
29 sparsely populated northwestern regions through power generation, while health burdens  
30 concentrate in the densely populated industrial manufacturing belt of central and northern China.  
31 Despite production-side divergences, we identify a notable alignment at the final production  
32 level, offering opportunities to narrow the energy intensity gap through supply-chain  
33 coordination. We simulate three convergence scenarios in which upstream producers in the  
34 nonmetal, metal, and power sectors adopt energy intensities of their downstream partners.  
35 These include full convergence (100% adoption) and two partial convergence scenarios (75%  
36 and 50% adoption), with the latter constrained by national benchmark performance. Full  
37 convergence reduces trade-related CO<sub>2</sub> emissions by 17% (491 Mt) and averts 19% of  
38 associated mortality ( $3.8 \times 10^4$  deaths). Partial convergence scenarios still deliver meaningful  
39 co-benefits. This demonstrates that supply-chain coordination offers pathways to reconciling  
40 production-side disparities and more balanced climate–health co-benefits in China.

41 **Keywords:** supply-chain coordination, climate-health co-benefits, regional disparity

42 **Synopsis Statement:** Coordinating provincial supply chains provides a strategic pathway to  
43 align climate mitigation with public health benefits in China.

44 **1. INTRODUCTION**

45 Addressing the dual challenges of climate change and air pollution-related health impacts  
46 remains a pressing priority for China.<sup>1-3</sup> Both challenges stem largely from shared sources—  
47 combustion processes and industrial activities—justifying the need for integrated mitigation of  
48 carbon dioxide (CO<sub>2</sub>) and air pollutant emissions.<sup>4</sup> Co-mitigation strategies offer substantial  
49 advantages by simultaneously addressing both issues more efficiently, while also delivering  
50 immediate health benefits that can help build public support—particularly given that the long-  
51 term gains of climate policies are often intangible.<sup>4,5</sup> As China nears the saturation point of end-  
52 of-pipe pollution control technologies, further emission reduction through conventional  
53 approaches is becoming increasingly constrained.<sup>6,7</sup> Consequently, strategies focusing on  
54 improvements in fuel efficiency, shifts towards renewable energy, and structural industrial  
55 upgrades are emerging as critical pathways for future air pollution control and climate  
56 mitigation.<sup>8-10</sup>

57 However, the effectiveness of co-mitigation efforts is complicated by divergent sectoral  
58 emission profiles and spatial distributions. While CO<sub>2</sub> emissions are predominantly  
59 concentrated in power generation and contribute to global climate impacts, air pollutants are  
60 mainly emitted by energy-intensive industries and residential sectors, exerting localized health  
61 effects that depend on population density, meteorological conditions, and atmospheric  
62 chemistry.<sup>11-13</sup> This spatial heterogeneity presents a significant challenge, as industrial  
63 agglomeration has concentrated polluting industries in particular regions—often densely  
64 populated—where economic development has driven the clustering of heavy industries.<sup>14</sup>  
65 Although large facilities in these areas are generally better equipped to implement advanced

66 end-of-pipe controls and energy efficiency measures than smaller operations,<sup>15</sup> they  
67 simultaneously generate pollution hotspots that disproportionately affect local populations.<sup>16</sup>

68 This complexity is further amplified by the structure of supply chains, which effectively  
69 redistribute emissions and associated health damages across regions. Economically developed  
70 provinces often outsource their emissions and health impacts to industrial clusters in less  
71 developed areas, creating a geographical mismatch between those who consume goods and  
72 those who bear the environmental and health burdens of production.<sup>17-19</sup> Approximately 25%  
73 of China's PM<sub>2.5</sub>-related deaths are linked to interprovincial trade, with emissions typically  
74 transferred from developed coastal provinces to interior regions where mitigation resources are  
75 limited.<sup>20</sup> This pattern not only weakens regional mitigation efforts but also exacerbates  
76 inequalities in health outcomes, thereby impeding progress toward several Sustainable  
77 Development Goals (SDGs), including reduced inequalities (SDG 10), good health and well-  
78 being (SDG 3), and climate action (SDG 13).<sup>21</sup>

79 The divergence between production-side emission patterns of carbon and air pollutants calls  
80 for greater attention to coordination at the supply-chain level in co-mitigation research. While  
81 production-oriented approaches have demonstrated considerable potential for delivering co-  
82 benefits,<sup>13,22,23</sup> studies focusing on co-benefits along supply chains remain limited. Recent  
83 studies have examined carbon emissions<sup>24-26</sup> and air pollution-related health impacts<sup>20,27-29</sup>  
84 embodied in interregional trade; few have provided an integrated, high-resolution assessment  
85 that captures the coupling between climate and health impacts within supply chains. Most  
86 existing health attribution studies predominantly employ scenario-based analyses or reduced-  
87 complexity models,<sup>20,28</sup> which either lack spatial resolution for source-specific contributions or

88 inadequately represent atmospheric physicochemical processes. A better understanding of how  
89 carbon emissions and health impacts may exhibit different spatial and sectoral patterns along  
90 supply chains is critical to inform effective co-mitigation strategy design.

91 To address these complex dynamics, we integrate input-output analyses with spatially explicit  
92 health impact assessments to examine how interprovincial trade in China redistributes both CO<sub>2</sub>  
93 emissions and air pollution-related health damages. Our high-resolution analytical framework,  
94 which incorporates harmonized emission inventories, evaluates polarization patterns of carbon  
95 emissions and health impacts, revealing the influence of industrial agglomeration and supply  
96 chain-mediated emission relocation. Crucially, we assess the potential co-benefits of reducing  
97 the energy intensities of trade partners to levels comparable to those of outsourcing provinces,  
98 identifying strategic opportunities for synergistic mitigation. By exploring the interplay among  
99 industrial structure, trade patterns, emissions, and health outcomes, our study provides a  
100 comprehensive framework for addressing the intertwined challenges of climate change and air  
101 pollution in China, with broader implications for other countries facing similarly complex  
102 supply chain dynamics.

103

## 104 **2. METHODS**

105 Our integrated analytical framework combines three main components to assess climate-health  
106 co-mitigation potential in China's interprovincial supply chains (Figure S1): (1) High-  
107 resolution adjoint modeling using the Community Multiscale Air Quality (CMAQ) v5.0 to  
108 quantify how location- and species-specific emissions contribute to PM<sub>2.5</sub>-related mortality  
109 nationwide; (2) Multi-regional input-output (MRIO) analysis using China's 2017 provincial

110 MRIO table to trace CO<sub>2</sub> emissions and health impacts through interprovincial trade flows; and  
111 (3) Scenario analysis evaluating co-benefits from aligning energy intensities across supply  
112 chain partners. This workflow enables us to identify spatial and sectoral patterns of burden  
113 redistribution and assess strategic opportunities for coordinated mitigation.

114 **2.1. Air Quality Modeling with the Adjoint Model.** We employ the adjoint<sup>30,31</sup> model of  
115 CMAQ<sup>32</sup> v5.0 to quantify the contributions of location- and species-specific air pollutant  
116 emissions to PM<sub>2.5</sub>-related premature deaths in China for the year 2017. CMAQ is a widely  
117 used chemical transport model (CTM) that simulates the transport and transformation of  
118 atmospheric pollutants and estimates their concentrations.<sup>32</sup> In this study, the CMAQ model is  
119 configured with the CB05 gas-phase chemistry mechanism and the AERO5 aerosol module.  
120 The adjoint model operates similarly to the CTM but in reverse, tracking the impact of a  
121 pollutant at receptor locations back to its emission sources through a cost function.<sup>30</sup> In our case,  
122 the cost function is the total number of premature deaths attributable to PM<sub>2.5</sub> exposure for  
123 China. Mortality estimates cover five major causes, including ischemic heart disease (IHD),  
124 cerebrovascular disease (stroke), chronic obstructive pulmonary disease (COPD), and lung  
125 cancer (LC) for adults over 25 years old, and acute lower respiratory illness for children under  
126 five. A single adjoint simulation provides the sensitivity of model output (e.g., PM<sub>2.5</sub>-related  
127 mortality) to emissions at all locations and times, without the need for multiple forward  
128 simulations with perturbed inputs. The adjoint approach has been extensively applied in  
129 backward sensitivity analysis, source attribution, data assimilation, and inverse modeling.<sup>33-35</sup>  
130 The CMAQ adjoint implementation includes multiphase aerosol-forming processes, which  
131 allows efficient and high-resolution source attribution of health impacts.<sup>31</sup> Using the adjoint

132 simulation, we quantify the contributions of emissions from seven species to PM<sub>2.5</sub>-related  
133 mortality, including organic carbon (OC), elemental carbon (EC), other primary PM<sub>2.5</sub>, sulfur  
134 dioxide (SO<sub>2</sub>), nitrogen oxides (NO<sub>x</sub>), ammonia (NH<sub>3</sub>), and volatile organic compounds  
135 (VOCs). The mathematical derivation of adjoint sensitivity analysis is presented in previous  
136 studies<sup>11,19</sup> and summarized in Text S1.

137 The modeling domain covers all of China with a horizontal resolution of 36 × 36 km (Figure  
138 S2) and 13 vertical layers extending up to ~16 km above the ground. Anthropogenic emissions  
139 are derived from the AiMa emission inventory (<http://www.aimayubao.com/>),<sup>36</sup> which  
140 categorizes eight sources (i.e., power generation, industry, residential, transportation,  
141 agriculture, solvent usage, fugitive dust, and fires).<sup>37,38</sup> The AiMa inventory provides  
142 constrained bottom-up emission data for China, integrating statistical data, ground  
143 measurements, and satellite observations. It has been extensively used and validated in previous  
144 modeling studies and air quality forecasting services in China.<sup>11,39,40</sup> Meteorological inputs are  
145 generated using the Weather Research Forecasting (WRF) model v3.4.1,<sup>41</sup> driven by global  
146 weather forecast products from the National Centres for Environmental Prediction (NCEP)  
147 Global Forecast System<sup>42</sup> at a spatial resolution of 0.5° × 0.5°.

148 To ensure robust exposure-response assessment, simulated concentrations of PM<sub>2.5</sub>, PM<sub>10</sub>, SO<sub>2</sub>,  
149 and NO<sub>2</sub> are evaluated against observations from 1,504 ground-based monitoring sites across  
150 China (Figures S3 and S4). The model successfully reproduces the spatial distribution of PM<sub>2.5</sub>  
151 concentration with a Pearson correlation coefficient (*r*) of 0.63, and performance metrics for all  
152 evaluated pollutants meet or approach recommended benchmarks, indicating reliable model  
153 performance.<sup>43,44</sup> In addition, the adjoint sensitivities are validated against forward sensitivities

154 derived from finite-difference and complex variable methods, showing consistent results.<sup>31</sup>

155 Further details on model evaluation are provided in Text S2.

156 **2.2. Emissions and Associated Health Impacts Embodied in the Supply Chains.** While  
157 AiMa provides better constrained model-ready emission inputs, it lacks the sectoral resolution  
158 required for MRIO analysis. We therefore employ the Global Emission Modeling System  
159 (GEMS),<sup>45,46</sup> which provides production-based emissions disaggregated by sector and fuel  
160 combinations (Table S1). To ensure consistency with our air quality modeling, GEMS sectoral  
161 emissions are harmonized with provincial totals from AiMa. The mapping between GEMS  
162 sectors and the MRIO sectoral classification is provided in Text S3. Notably, direct household  
163 emissions from residential fossil/biomass combustion for cooking and heating, as well as  
164 emissions from private cars, are excluded from the MRIO analysis since they do not enter  
165 economic supply chains.

166 Second, we attribute emissions emitted in each region (i.e., direct emitter) to both final  
167 producers<sup>47–49</sup> (who produce the finished products using local or imported intermediate inputs)  
168 in supply chains and final consumers<sup>47,49</sup> (who ultimately consume the finished products).

169 Environmentally extended MRIO models, based on input-output tables that capture exchanges  
170 within and among regions, have been widely applied to trace environmental burdens along  
171 increasingly interconnected supply chains.<sup>26–29</sup> In this study, we use the 2017 multiregional  
172 input-output table from the China Emission Accounts and Datasets (CEADs) database<sup>50</sup> to  
173 quantify emissions embodied in China's supply chains. The MRIO table covers 31 mainland  
174 provincial-level administrative divisions (excluding Macao, Hong Kong, and Taiwan) and 42  
175 economic sectors (Table S2). Emissions embodied in international imports for domestic

176 consumption are not considered, as this study focuses on interprovincial trade. By combining  
177 adjoint sensitivities with emissions related to economic activities (i.e., final producer or final  
178 consumer), we trace PM<sub>2.5</sub>-related mortality along interprovincial supply chains. Further  
179 methodological details are provided in Texts S4 and S5.

180 A comprehensive uncertainty analysis is conducted using 10,000 Monte Carlo simulations,  
181 incorporating uncertainties from emission inventories and concentration-response functions.  
182 The associated uncertainty ranges for CO<sub>2</sub> emissions and PM<sub>2.5</sub>-related premature deaths are  
183 reported throughout the study, with full details available in Text S6.

184 **2.3. Disparities in Carbon Emissions and Health Damage.** To facilitate direct interprovincial  
185 comparison of disparity in carbon emissions and health damage from the final production  
186 perspective, we introduce two normalized indices: the Trade-related carbon emission disparity  
187 index (*TCI*) and the Trade-related health damage disparity index (*THI*), which can be expressed  
188 as follows:

$$189 \quad TCI^r = \frac{EEI^r - EEE^r}{EEI^r + EEE^r} \quad (1)$$

$$190 \quad THI^r = \frac{MEI^r - MEE^r}{MEI^r + MEE^r} \quad (2)$$

191 where  $EEI^r$  and  $MEI^r$  are emissions and mortality embodied imports for province  $r$ ,  
192 respectively, while  $EEE^r$  and  $MEE^r$  are emissions and mortality embodied in exports for  
193 province  $r$ , respectively. Detailed calculations are provided in Text S7. For both indices (*TCI*  
194 and *THI*), the values range from  $-1$  (strong net receiving regions of emissions/health burdens)  
195 to  $1$  (strong net outsourcing regions). Throughout this study, “export” and “import” refer to  
196 interprovincial trade unless noted, whereas “international export” refers to China’s exports to

197 the rest of the world.

198 **2.4. Co-Mitigation via Sectoral Energy Intensity Convergence.** We define potential  
199 reductions in both CO<sub>2</sub> emissions and PM<sub>2.5</sub>-related health damages achievable through supply-  
200 chain coordination of energy intensities. Energy intensity is measured as energy consumption  
201 per unit of physical output, expressed in tonnes of coal equivalent (tce). To demonstrate the  
202 potential of supply-chain coordination for co-mitigation, we quantify emission and health  
203 benefits for three sectors—nonmetal, metal, and energy generation—that not only contribute  
204 most to these impacts but also have available physical output data.<sup>20,25</sup> Energy intensities for  
205 these sectors are measured as tce per 100 tonnes of cement, tce per 100 tonnes of steel, and tce  
206 per 10<sup>5</sup> kWh of electricity, respectively (Figure S5). Physical output data are obtained from the  
207 China Statistical Yearbook 2018<sup>51</sup> and the China Energy Statistical Yearbook 2018<sup>52</sup>, and energy  
208 consumption data are derived from activity data underlying the GEMS inventory.

209 Emission reduction through supply-chain coordination refers to the reduction embodied in a  
210 province's imports for final production, achieved when downstream provinces with lower  
211 energy intensities influence their upstream suppliers to adopt improved performance levels.  
212 This approach preserves MRIO relationships without altering inter-sectoral technical  
213 coefficients. We calculate the supply-chain coordination potential for each province serving as  
214 a downstream final production hub across all provinces in mainland China. Emission reduction  
215 ( $\Delta E^{r,s}$ ) and health benefits ( $\Delta M^{r,s}$ ) in imports of goods by province  $s$  from province  $r$  are  
216 calculated as:

$$217 \Delta E^{r,s} = \sum_{m \in \{nonmetal, metal, power\}} E_m^{r,s} \cdot \left( 1 - \frac{w'_{r,m}}{w_{r,m}} \right) \quad (3)$$

218

$$\Delta M^{r,s} = \sum_{m \in \{nonmetal, metal, power\}} M_m^{r,s} \cdot \left(1 - \frac{w'_{r,m}}{w_{r,m}}\right) \quad (4)$$

219 where  $E_m^{r,s}$  and  $M_m^{r,s}$  are emissions and associated mortality that occur in province  $r$  for sector  
 220  $m$  when producing intermediate goods consumed in province  $s$ , respectively.  $w_{r,m}$  and  $w'_{r,m}$   
 221 are the original and adjusted energy intensities of sector  $m$  in province  $r$ , respectively.

222 We examine three coordination scenarios, with adjusted energy intensity  $w'_{r,m}$  defined as:

223

$$w'_{r,m} = \begin{cases} w_{s,m} & , \text{if } w_{s,m} < w_{r,m}, 100\% \text{ coordination} \\ \max(w_{s,m}, q_{25}) & , \text{if } w_{s,m} < w_{r,m}, 75\% \text{ coordination} \\ \max(w_{s,m}, q_{50}) & , \text{if } w_{s,m} < w_{r,m}, 50\% \text{ coordination} \\ w_{r,m} & , \text{otherwise} \end{cases} \quad (5)$$

224 where  $w_{s,m}$  is the energy intensity of sector  $m$  in province  $s$ .  $q_{25}$  and  $q_{50}$  represent the 25th and  
 225 50th percentiles of the provincial energy intensity distribution for sector  $m$ , respectively (Figure  
 226 S6). Under full coordination, upstream provinces completely adopt the downstream province's  
 227 cleaner technology when downstream provinces operate more efficiently than their upstream  
 228 suppliers, representing an optimal case. Under partial coordination, technology transfer is  
 229 constrained either by the downstream province's performance or national benchmarks,  
 230 reflecting realistic limitations in achieving complete convergence.

231

232 **3. RESULTS and DISCUSSION**

233 **3.1. Sectoral Shift in CO<sub>2</sub> Emissions and PM<sub>2.5</sub>-Related Premature Deaths along Supply  
 234 Chains.** In 2017, China emitted 10,495 Mt (95% CI: 8,279–13,121) of anthropogenic CO<sub>2</sub>,  
 235 along with 7.8 Mt (95% CI: 3.5–15.2) of primary PM<sub>2.5</sub>, 10.8 Mt (95% CI: 5.4–19.5) of SO<sub>2</sub>,  
 236 22.4 Mt (95% CI: 17.9–27.6) of NO<sub>x</sub>, and 11.0 Mt (95% CI: 8.6–13.9) of NH<sub>3</sub>. Notably, 91%  
 237 of China's anthropogenic CO<sub>2</sub> emissions and a substantial share of air pollutant emissions—

238 ranging from 63% for PM<sub>2.5</sub> to 94% for NH<sub>3</sub>—are related to economic activities along supply  
239 chains, rather than residential direct energy consumption (Figure S7). Using an adjoint-based  
240 source attribution approach, we link these supply chain-related emissions to approximately 9.9  
241  $\times 10^5$  premature deaths (95% CI:  $5.9 \times 10^5$ – $1.6 \times 10^6$ ) nationwide. For the health co-benefit  
242 assessment, we exclude the 16% contribution from NH<sub>3</sub> emissions and 5% contribution from  
243 VOCs (Figure S8), as NH<sub>3</sub> primarily originates from fertilizer application and livestock  
244 management while VOCs largely come from solvent use and fugitive emissions (Figure S9).

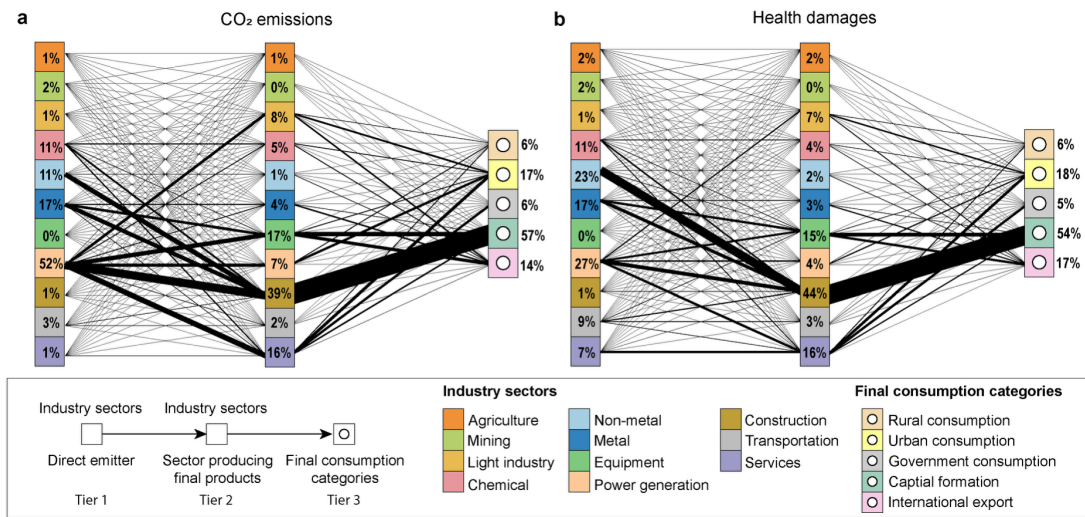
245 Mapping emissions and associated health damages across 42 economic sectors reveals  
246 substantial divergences in production-side contributions to CO<sub>2</sub> emissions and PM<sub>2.5</sub>-related  
247 premature deaths. Power generation accounts for over half of production-based CO<sub>2</sub> emissions  
248 but contributed to less than one-third of PM<sub>2.5</sub>-related deaths (Figure 1). This imbalance is  
249 largely due to the widespread implementation of stringent emission control technologies in  
250 power plants.<sup>53</sup> These controls limit power generation’s contribution to only 20% of embodied  
251 primary PM<sub>2.5</sub> emissions and 39% of secondary precursor emissions (SO<sub>2</sub> and NO<sub>x</sub>) (Figure  
252 S10). In contrast, the three major heavy industries—chemical, metal, and nonmetal  
253 production—exhibit varied contribution patterns. While chemical and metal production make  
254 relatively balanced contributions to both CO<sub>2</sub> emissions and PM<sub>2.5</sub>-related premature deaths  
255 (approximately 11% and 23%, respectively), nonmetal production stands out by contributing  
256 nearly a quarter of health damages despite its relatively lower CO<sub>2</sub> contributions. Additionally,  
257 transportation and service sectors show higher relative contributions to health damages than to  
258 CO<sub>2</sub> emissions.

259 These sectoral imbalances present challenges for production-side co-mitigation strategies.

260 When shifting from a production-side to a final production-side perspective, we observe that  
261 CO<sub>2</sub> emissions and associated health damages driven by the same final production sector often  
262 pass through different upstream production pathways. For example, while 41% of CO<sub>2</sub>  
263 emissions attributed to construction demand originate from power generation, 44% of the  
264 associated premature deaths are primarily caused by emissions from nonmetal production.  
265 Similarly, for equipment and services demand, power generation is the main source of CO<sub>2</sub>  
266 emissions, whereas the metal and services sectors are the primary contributors to health impacts.  
267 This misalignment between sectors driving carbon emissions and those causing health damages  
268 complicates efforts to achieve balanced co-benefits through production-focused interventions  
269 alone.

270 Despite these production-side divergences, our analysis identifies strategic coordination  
271 opportunities at the supply-chain level. Both CO<sub>2</sub> emissions and PM<sub>2.5</sub>-related premature deaths  
272 embodied in supply chains are driven by common underlying final consumption categories.  
273 Over half of these CO<sub>2</sub> emissions and health impacts can be attributed to a single category—  
274 capital investment—especially through construction and equipment demand. This pattern  
275 indicates the central role of China's real estate industry and infrastructure projects in driving  
276 both climate change and air pollution-related health damages.<sup>20,25,54</sup> Together, the top three final  
277 production sectors—construction, equipment, and services—account for 94% of embodied CO<sub>2</sub>  
278 emissions and premature deaths driven by capital investment. Beyond capital investment,  
279 international export also plays a significant role, contributing 36% of both CO<sub>2</sub> emissions and  
280 premature deaths embodied in equipment demand. This alignment between CO<sub>2</sub> emissions and  
281 health impacts at the final production level demonstrates how consumption-driven demand

282 patterns ultimately shape both climate change and air pollution-related health damages, offering  
 283 strategic intervention points along supply chains where co-benefits can be achieved.



284  
 285 **Figure 1. Sectoral flow patterns of CO<sub>2</sub> emissions and health damages in 2017.** Sankey diagrams  
 286 show the flows of (a) CO<sub>2</sub> emissions and (b) PM<sub>2.5</sub>-related premature deaths through China's supply  
 287 chains, traced from upstream production sectors (Tier 1, left), through sectors producing final goods and  
 288 services (Tier 2, middle), to final demand categories (Tier 3, right). Line thickness indicates the relative  
 289 magnitude of emission or premature deaths transferred between tiers. Percentages show the share of  
 290 impacts attributed to each sector at each tier. "Capital formation" includes both fixed capital investment  
 291 and capital inventory. For clarity, the original 44 economic sectors are aggregated into 11 broad categories  
 292 (see Table S2).

293

### 294 3.2. Relocation of CO<sub>2</sub> Emissions and PM<sub>2.5</sub>-Related Premature Deaths in Key Sectors.

295 Interprovincial trade between production-side regions and final production-side regions  
 296 accounts for 35% of the national total CO<sub>2</sub> emissions (3,682 Mt, 95% CI: 2905–4603) and 20%  
 297 of PM<sub>2.5</sub>-related deaths ( $2.8 \times 10^5$ , 95% CI:  $1.6 \times 10^5$ – $4.9 \times 10^5$ ). Sector- and provincial-specific  
 298 analyses reveal that these trade-embodied impacts are highly concentrated, with nearly half of  
 299 both CO<sub>2</sub> emissions and PM<sub>2.5</sub>-related deaths linked to just 3% of all trade flows (Figure S11),  
 300 primarily involving the nonmetal, metal, and power generation sectors. Spatially, final  
 301 production demand from economically advanced provinces drives distinct sectoral relocation

302 patterns, each governed by different spatial mechanisms (Figure 2).

303 Proximity-driven relocation characterizes the nonmetal sector, where emission relocation is

304 largely confined to geographically adjacent provinces due to high transport costs of bulk

305 materials such as cement and bricks. For instance, Shanghai's demand leads to significant CO<sub>2</sub>

306 emission relocation to neighboring Zhejiang, while Jiangsu's demand causes the largest health

307 damage relocation to adjacent Anhui. Similarly, Beijing externalizes a considerable portion of

308 nonmetal production to Hebei. This proximity-driven outsourcing has fostered industrial

309 clusters in surrounding provinces that often enforce comparatively lenient environmental

310 regulations relative to economic hubs like Zhejiang, Jiangsu, and Guangdong.<sup>55</sup> These

311 regulatory disparities translate into lower pollution control efficiency, generating

312 disproportionate health burdens relative to carbon footprints. Provinces such as Anhui and

313 Hebei, which specialize in energy- and emission-intensive processes like cement clinker

314 production, experience disproportionate health damage, with their shares of relocated PM<sub>2.5</sub>-

315 related mortality exceeding their shares of relocated CO<sub>2</sub> emissions by 60% and 73%,

316 respectively. In contrast, Zhejiang, equipped with more advanced pollution control technologies,

317 exhibits a 40% lower share of relocated mortality compared to its corresponding CO<sub>2</sub> emissions.

318 The metal sector displays more spatially dispersed relocation patterns while maintaining similar

319 efficiency disparities. Zhejiang and Guangdong, as major manufacturing hubs producing final

320 metal products, drive production in upstream regions. Together, they account for 31% of all

321 relocated CO<sub>2</sub> emissions and PM<sub>2.5</sub>-related mortality in the metal sector, with their demand

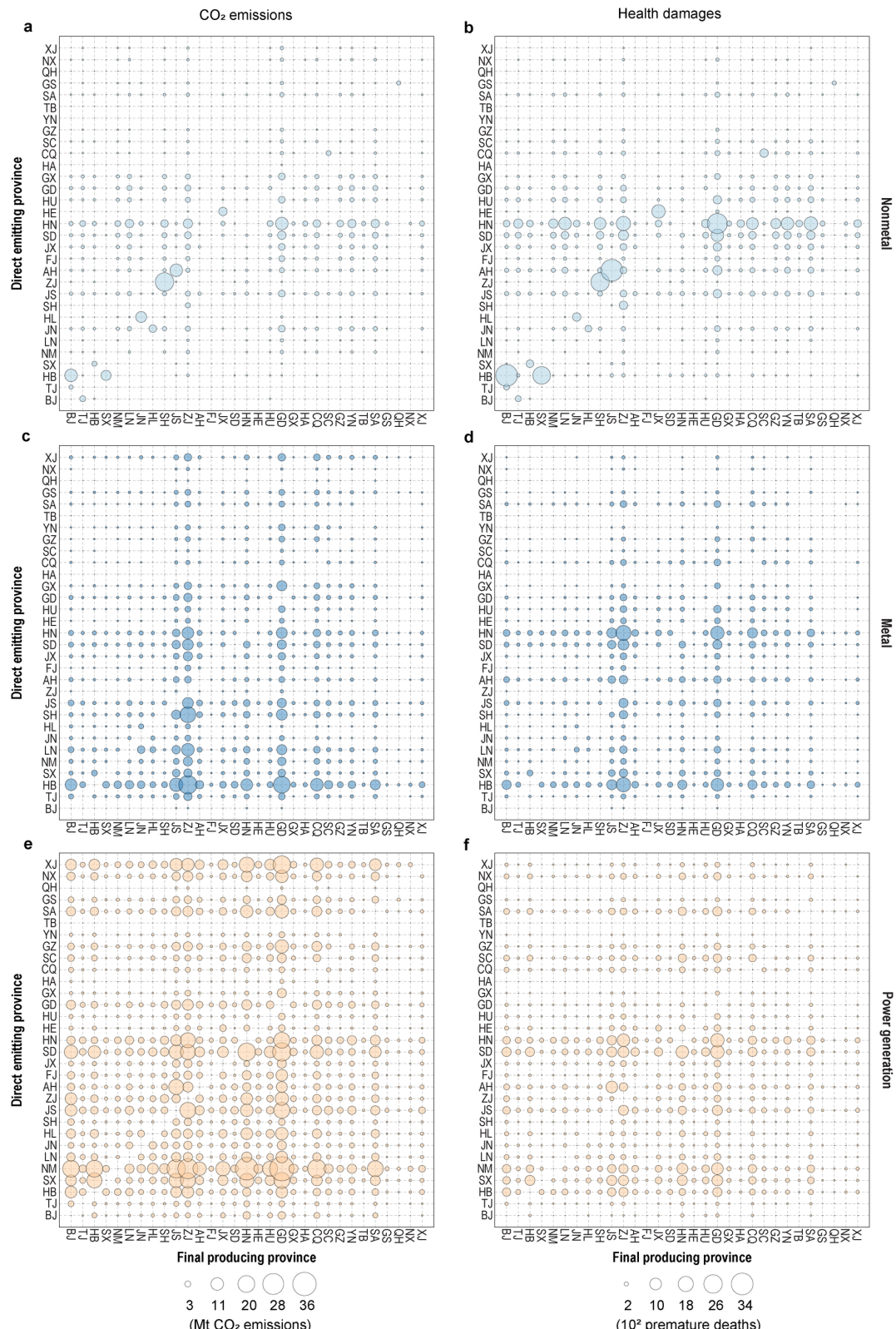
322 influencing production across 29 of China's 30 mainland provinces. Relocated impacts

323 concentrate in the leading iron and steel-producing provinces. These production regions exhibit

324 significant heterogeneity in pollution control efficiency. Hebei accounts for 19% of relocated  
325 CO<sub>2</sub> emissions and 16% of health impacts, maintaining relatively balanced ratios. However,  
326 Henan contributes 15% of relocated mortality despite generating only 6% of relocated CO<sub>2</sub>  
327 emissions. This disparity reflects significant heterogeneity in pollution control technologies,  
328 particularly in the emission-intensive sintering process.<sup>56</sup> Weaker emission standards in Henan  
329 result in higher pollutant emissions—and consequently greater health damages—per unit of  
330 CO<sub>2</sub> emitted (Figure S12).

331 The power generation sector exhibits a resource-driven spatial pattern shaped by energy  
332 resource distribution and grid infrastructure. Final production demand spans both developed  
333 provinces (e.g., Beijing, Jiangsu, Zhejiang, and Guangdong) and industrial regions (Henan,  
334 Hebei, and Shaanxi). However, the geography of power production creates pronounced health  
335 impact disparities. Roughly 25% of CO<sub>2</sub> emissions (525 Mt, 95% CI: 414–656) and 33% of  
336 associated premature deaths ( $3.0 \times 10^4$ , 95% CI:  $1.7 \times 10^4$ – $5.3 \times 10^4$ ) are relocated to densely  
337 populated industrial provinces, including Hebei, Henan, Shandong, and Jiangsu. In contrast,  
338 another 25% of CO<sub>2</sub> emissions are externalized to energy-rich northwestern provinces—Inner  
339 Mongolia, Xinjiang, and Ningxia—but generate only  $1.1 \times 10^4$  premature deaths (95% CI:  $6.1$   
340  $\times 10^3$ – $1.9 \times 10^4$ ). The stark contrast is primarily driven by demographic differences—the  
341 average population density in the four eastern industrial provinces exceeds that in the three  
342 northwestern provinces by a factor of 29. Our adjoint analysis confirms that the emission-  
343 weighted sensitivity of primary PM<sub>2.5</sub> and its precursors in Henan is 165% to 420% higher than  
344 that in Inner Mongolia and Xinjiang, respectively (Figure S13).

346 **Figure 2. Relocation of CO<sub>2</sub> emissions and health damages driven by interprovincial trade across**  
 347 **key industrial sectors.** Bubble plots illustrate the relocation of impacts across provinces, with each panel  
 348 representing a specific sector: (a–b) nonmetal, (c–d) metal, and (e–f) power generation. Left panels (a,  
 349 c, e) show CO<sub>2</sub> emissions, while right panels (b, d, f) show PM<sub>2.5</sub>-related premature deaths. Each circle  
 350 represents the impacts that occurred in the producing province (y-axis), induced by demand from the



351 final producing province ( $x$ -axis). Circle size is proportional to the magnitude of transferred impact, as  
352 indicated in the legends below. Local consumption impacts (i.e., those on the diagonal from lower left to  
353 upper right) are set as zeros and not displayed. Province abbreviations: BJ, Beijing; TJ, Tianjin; HB,  
354 Hebei; SX, Shanxi; NM, Inner Mongolia; LN, Liaoning; JL, Jilin; HL, Heilongjiang; SH, Shanghai; JS,  
355 Jiangsu; ZJ, Zhejiang; AH, Anhui; FJ, Fujian; JX, Jiangxi; SD, Shandong; HN, Henan; HE, Hubei; HU,  
356 Hunan; GD, Guangdong; GX, Guangxi; HA, Hainan; CQ, Chongqing; SC, Sichuan; GZ, Guizhou; YN,  
357 Yunnan; TB, Tibet; SA, Shaanxi; GS, Gansu; QH, Qinghai; NX, Ningxia; XJ, Xinjiang.

358

359 **3.3. Divergent Polarization of CO<sub>2</sub> Emissions and PM<sub>2.5</sub>-Related Premature Deaths.** To  
360 systematically assess how sectoral emission relocations translate into broader provincial  
361 disparities, we developed two complementary metrics: the trade-related carbon emission  
362 disparity index (TCI) and the trade-related health damage disparity index (THI). These indices  
363 evaluate whether a province is a net importer or exporter of environmental burdens, normalized  
364 from -1 (strong exporter) to 1 (strong importer), allowing for direct cross-provincial  
365 comparison.

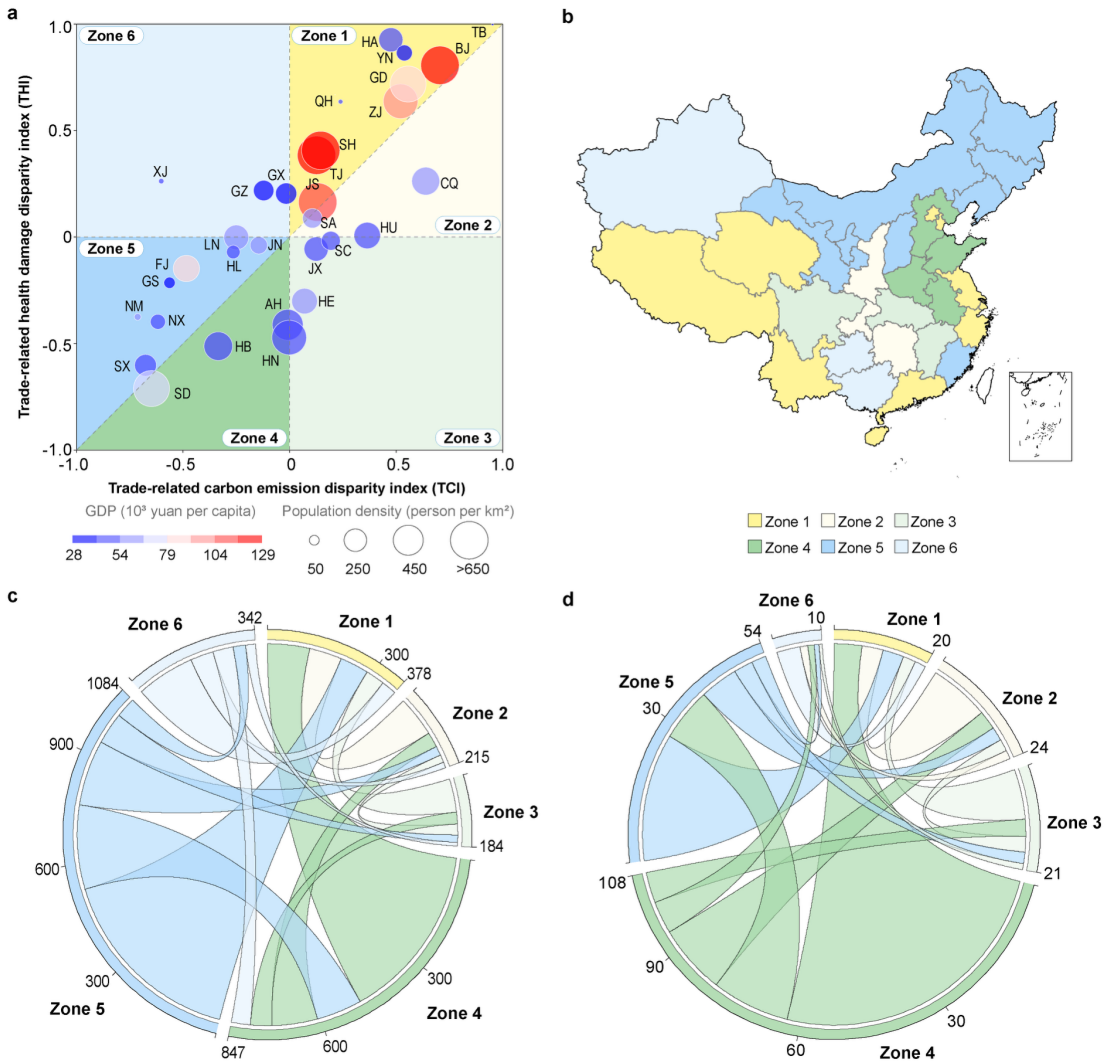
366 By plotting provinces based on their TCI and THI scores (Figure 3a), we identified six distinct  
367 zones characterizing the spatial distribution of carbon and health burden transfer. Most  
368 provinces cluster in the upper-right and lower-left quadrants (Zones 1, 2, 4, and 5), indicating  
369 a systematic pattern of burden relocation through interprovincial trade. Provinces that function  
370 as final production hubs in our sectoral analysis—Beijing, Shanghai, Zhejiang, and  
371 Guangdong—cluster in Zone 1 along the 1:1 line, reflecting high TCI and THI scores. These  
372 provinces capture high added value through final goods production while driving demand for  
373 raw materials and intermediate goods from other regions. Their supply-chain networks generate  
374 comparable relocations of both carbon emissions and health impacts, indicating aligned burden  
375 transfer patterns. Interestingly, several less-developed provinces—including Hainan, Yunnan,

376 and Tibet—also fall within Zone 1, despite their relatively minor contributions to national totals  
377 (Figure S14). These provinces exhibit high dependence on imports due to increasing  
378 consumption and limited local production capacity.<sup>20,25</sup> Given their import dependence,  
379 development-oriented policies are needed to promote sustainable local production and reduce  
380 reliance on emission-intensive imports.

381 Zone 2 comprises provinces with decoupled carbon and health burden profiles. These provinces  
382 typically import electricity and raw materials while exporting manufactured goods,<sup>20,25</sup> creating  
383 asymmetric environmental burden patterns. Though their TCI scores are positive, their THI  
384 scores are comparatively lower, as local manufacturing emissions offset the health gains  
385 achieved through outsourcing. Chongqing exemplifies this trend, with a TCI of 0.6 but a THI  
386 of only 0.2, reflecting how local topography and population density intensify health impacts  
387 from its industrial activities.<sup>57</sup>

388 Burden-bearing provinces exhibit diverging patterns, rather than aligning along the 1:1 line.  
389 Zone 4 provinces—concentrated in North and Central China (Figure 3b)—form a densely  
390 populated industrial manufacturing corridor shaped by historical infrastructure development,  
391 market accessibility, and labor availability.<sup>58</sup> Provinces with manufacturing specialization and  
392 less stringent pollution controls—particularly Henan and Anhui—fall into this zone with THI  
393 scores around -0.5 but TCI scores near zero. This pattern indicates these provinces shoulder  
394 disproportionate health burdens relative to their net carbon emissions, consistent with the  
395 pollution control efficiency disparities previously discussed. In contrast, Zone 5 includes  
396 sparsely populated northwestern regions, showing significant carbon leakage but minimal  
397 health burden spillover, largely due to low population exposure.

398 Chord diagrams (Figure 3c,d) further visualize this divergence. The dominant carbon flow runs  
399 from Zone 5 to Zone 1, with approximately 530 Mt (95% CI: 418–662) of CO<sub>2</sub> (17% of total  
400 interprovincial flows). In terms of health impacts, the primary flow is from Zone 4 to Zone 1,  
401 transferring approximately  $6.3 \times 10^4$  premature deaths (95% CI:  $3.5 \times 10^4$ – $1.1 \times 10^5$ ), or 27%  
402 of trade-related mortality. This single pathway accounts for more than twice the number of  
403 deaths exported from Zone 5 to Zone 1. Although CO<sub>2</sub> emissions and health impacts stem from  
404 different burden-bearing zones, they converge at a common outsourcing destination—Zone 1.  
405 These patterns reveal how final production activity in economically advanced provinces creates  
406 distinct spatial footprints for carbon and health burdens, with important implications for  
407 understanding coordination opportunities across China’s supply-chain networks.



408

409 **Figure 3. Polarization patterns in CO<sub>2</sub> emissions and health damages in China.** (a) Province-level  
 410 classification based on the trade-related carbon emission disparity index (TCI; x-axis) and the trade-  
 411 related health damage disparity index (THI; y-axis). TCI and THI represent normalized differences  
 412 between emissions (or health impacts) embodied in imports and exports. Circle size indicates population  
 413 density; circle color indicates GDP per capita (from dark blue for less developed to dark red for more  
 414 developed provinces). Province abbreviations follow Figure 2. (b) Spatial distribution of provinces by  
 415 zone classifications corresponding to panel (a). (c) Chord diagram showing major interregional CO<sub>2</sub>  
 416 emission transfers between zones. Line color represents the exporting zone, and line width indicates  
 417 transferred volume (in Mt CO<sub>2</sub>). (d) same as (c), but for PM<sub>2.5</sub>-related premature deaths (in thousands).

418 **3.4. Co-mitigation Opportunities through Supply-Chain Energy Intensity Coordination.**

419 Disparities in energy intensity are a key driver of the geographic and sectoral polarization of  
420 carbon emissions and associated health burdens.<sup>59,60</sup> Provincial energy intensities range from  
421 roughly twofold differences in power generation to more than 50-fold gaps in the metal sector  
422 (Figure S5). Power generation shows relatively smaller variation but still follows a regional  
423 divide, with provinces within the Northeast China Power Grid (Liaoning, Jilin, and  
424 Heilongjiang) exhibiting notably higher intensities. Developed coastal provinces consistently  
425 exhibit lower energy intensities compared to less-developed inland provinces. Major producers,  
426 such as Hebei for steel, Anhui for cement, and Inner Mongolia for electricity, exhibit  
427 intermediate energy intensity levels. These intensity gaps between final production hubs and  
428 their upstream supplier regions amplify trade-driven emission relocation and associated health  
429 burdens, revealing substantial potential for targeted intervention.

430 To quantify these opportunities, we simulate scenarios in which upstream producers adopt  
431 cleaner technologies through supply-chain coordination with the advanced provinces they serve.  
432 This reflects documented mechanisms of technology diffusion and knowledge spillovers when  
433 production regions are integrated into supply networks anchored by economically developed  
434 hubs.<sup>61–63</sup> We examine three convergence scenarios with varying degrees of adoption. Full  
435 convergence (100%) assumes complete alignment with downstream partners, while partial  
436 convergence (75% and 50%) imposes limits based on national benchmark performance (see  
437 Section 2.4).

438 Full convergence reduces trade-related CO<sub>2</sub> emissions from nonmetal, metal, and power  
439 generation sectors by 17% (491 Mt), and avoids 19% of the associated premature deaths (3.8 ×

440  $10^4$ ) (Figure 4a). Critically, partial convergence scenarios still deliver meaningful gains, with  
441 75% convergence achieving 364 Mt CO<sub>2</sub> reduction and  $2.8 \times 10^4$  avoided deaths, while 50%  
442 convergence yielding 213 Mt CO<sub>2</sub> reduction and  $1.3 \times 10^4$  avoided deaths, respectively. These  
443 findings demonstrate that supply-chain coordination offers viable pathways to co-benefits, even  
444 when technology transfer faces realistic constraints.

445 The spatial distribution of benefits reflects the burden-shifting patterns documented in Section  
446 3.3 and remains broadly consistent across scenarios (Figures 4b and S15). CO<sub>2</sub> reduction  
447 concentrates in northwestern and northeastern energy-supplying regions (Zone 5), while health  
448 benefits concentrate in densely populated central and northern provinces (Zone 4). This  
449 geographic divergence underscores how supply-chain coordination can simultaneously address  
450 carbon leakage to remote regions and health burden concentration in industrial corridors.

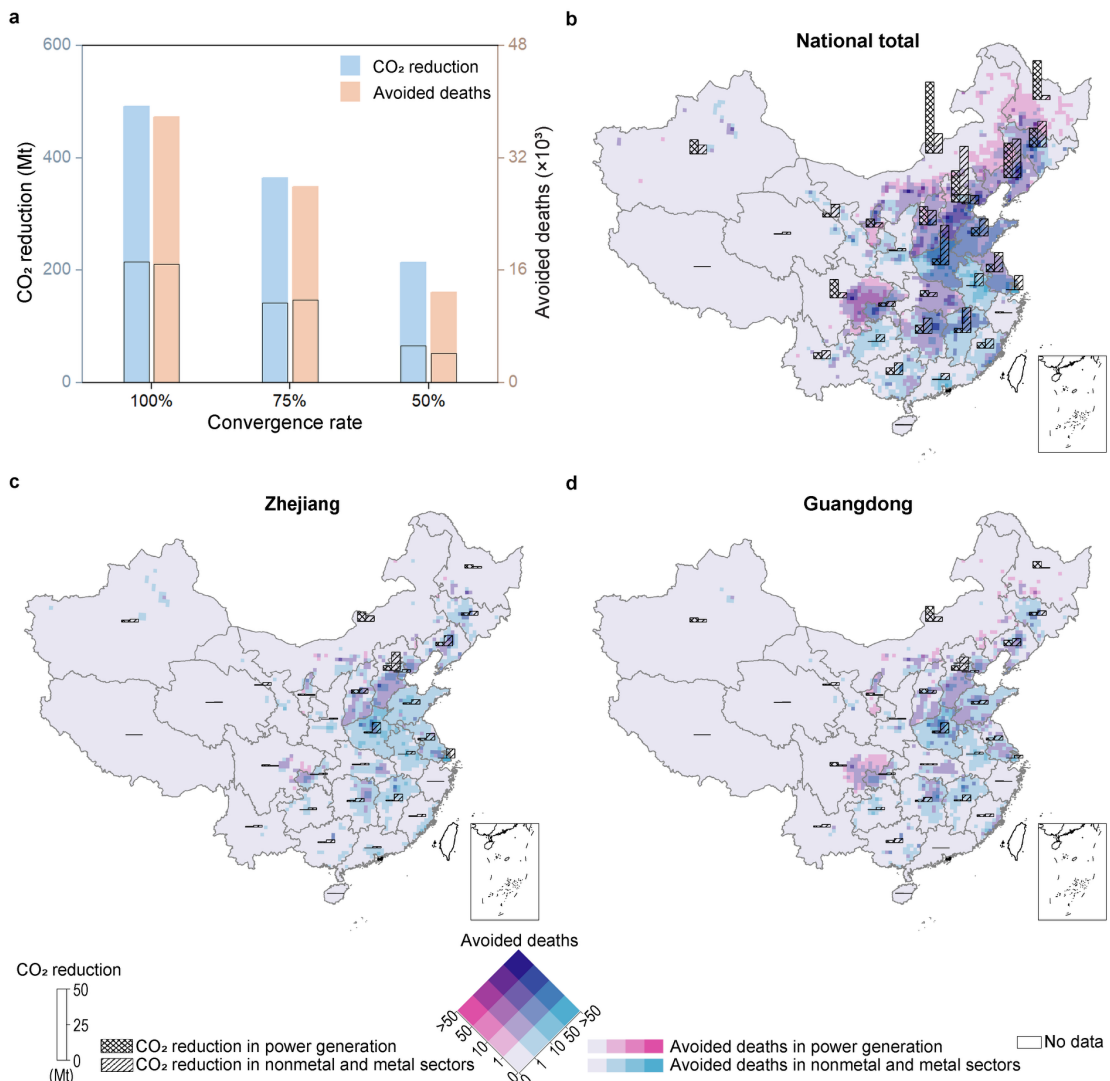
451 Sectoral priorities vary by coordination relationship, informing targeted technology transfer  
452 strategies. In Xinjiang, Ningxia, and Inner Mongolia—the major northwestern provinces  
453 supplying electricity to advanced coastal hubs—power sector improvements dominate potential  
454 co-benefits. For instance, reducing energy intensity in Inner Mongolia’s power generation  
455 could yield CO<sub>2</sub> reduction more than three times greater than that from industrial upgrades  
456 (nonmetal and metal). Conversely, in densely populated industrial provinces such as Hebei,  
457 improvements in the nonmetal and metal sectors deliver greater combined climate-health  
458 benefits due to higher exposure levels. Across most southern provinces, industrial sector  
459 improvements contribute more to CO<sub>2</sub> reduction than power-sector interventions, reflecting  
460 regional differences in industrial structure and electricity sourcing.

461 A small number of provinces can leverage their supply-chain influence to generate  
462 disproportionate co-benefits nationwide. Zhejiang and Guangdong emerge as the two most  
463 influential final production hubs, together accounting for about 44% of total achievable co-  
464 benefits under full convergence and about one-third under partial convergence (Figure 4a).

465 Their pathways to impact, however, show notable differences (Figure 4c,d). Zhejiang-driven  
466 coordination primarily reduces CO<sub>2</sub> emissions through nonmetal and metal sector  
467 improvements in proximate regions (Shanghai and Jiangsu) within the Yangtze River Delta and  
468 northern industrial provinces (e.g., Hebei and Liaoning). Guangdong, while achieving smaller  
469 reductions in these nearby regions, exerts broader geographical influence through long-distance  
470 supply chains. For example, Guangdong-driven collaboration yields substantial CO<sub>2</sub> reduction  
471 in Inner Mongolia and health benefits in Sichuan Basin and Ningxia, predominantly via power  
472 sector pathways. These complementary patterns suggest that effective strategies should  
473 capitalize on the different geographic and sectoral reach of these final production hubs.

474 Spatially explicit analysis at the grid level reveals that even within provinces, strategically  
475 targeted interventions can maximize efficiency of technology transfer investments. In Inner  
476 Mongolia, energy intensity reduction in eastern and central areas near population centers  
477 provides far greater health benefits than comparable actions in the sparsely populated western  
478 region. Similarly, in Hebei, southern industrial cities, such as Handan, Xingtai, and  
479 Shijiazhuang, emerge as high-priority intervention targets. Moreover, collaboration through  
480 different sectoral pathways produces spatially distinct benefit distribution patterns within  
481 provinces. In Shandong, for example, Guangdong-driven coordination generates greater health  
482 benefits in the southwestern region through power sector improvement, but produces larger

483 gains in other parts of the province through industrial improvements.



484

485 **Figure 4. Co-mitigation potential from narrowing sectoral energy intensity gaps along provincial**  
486 **supply chains in China.** (a) National total co-benefits under three convergence scenarios (100%, 75%,  
487 and 50%), in which upstream provinces are assumed to improve their sectoral energy intensity toward  
488 convergence benchmarks. Contributions from Zhejiang and Guangdong, the top two influential final  
489 production hubs, are highlighted with black boxes. (b-d) Reduction in CO<sub>2</sub> emissions (Mt, vertical bars)  
490 and avoided PM<sub>2.5</sub>-related premature deaths (colored background) for supply chains driven by the  
491 national total (b) and the top two provinces—Zhejiang (c) and Guangdong (d)—under the 100%  
492 convergence scenario. Results are shown by two sectoral categories: power generation and the industrial  
493 sectors of nonmetal and metal.

494

495 **3.5. Discussion and Environmental Implications.** Our integrated framework reveals the  
496 pivotal role of final producers in achieving climate-health co-mitigation. While production-side

497 emissions are spatially and sectorally dispersed, the final production demand driving these  
498 impacts is highly concentrated. This convergence pattern, obscured in previously separated  
499 analyses,<sup>20,25,26</sup> establishes final producers as critical coordination nodes. Furthermore, our  
500 high-resolution adjoint modeling shows that health impacts of these relationships vary  
501 substantially by location, depending on population exposure and regulation stringency. Hence,  
502 sourcing decisions directly determine both emission volumes and associated health impacts.  
503 This leverage can be exercised through strategic supplier selection and improvement initiatives,  
504 for which precedents already exist.

505 Evidence of final producers' coordination capacity spans multiple governance contexts. Apple's  
506 Supplier Clean Energy Program requires manufacturing partners to procure 100% renewable  
507 electricity and facilitate joint clean energy investments through mechanisms like the China  
508 Clean Energy Fund.<sup>64</sup> Under the Clean Development Mechanism, multinational companies  
509 have promoted energy efficiency among upstream partners in emerging economies by offering  
510 financial and technological support in exchange for carbon reduction credits.<sup>65</sup> Final producers  
511 have also coordinated technology diffusion by establishing common standards. Zhejiang's ISO  
512 50001 supplier certification program exemplifies how final producers can standardize  
513 efficiency practices across upstream partners, achieving an estimated 26% reduction in energy  
514 intensity.<sup>66</sup> Cross-firm R&D consortia enable collaborative development of technologies such  
515 as hydrogen-based direct reduction for iron ore processing, projected to reduce energy intensity  
516 by about 40% at marginal abatement costs below near-term carbon price forecasts.<sup>67</sup> At the  
517 regional level, the Beijing-Tianjin-Hebei coordination framework illustrates how final  
518 production hubs can drive upstream industrial transformation.<sup>68</sup> Beijing and Tianjin coordinate

519 emission reduction in Hebei through technical assistance and ecological compensation  
520 programs, facilitating large-scale phaseout of outdated crude steel capacity.<sup>69–71</sup> These examples  
521 demonstrate coordination feasibility across corporate, sectoral, and regional scales. Achieving  
522 the 17% emission and 19% mortality reduction identified in our full convergence scenario  
523 would require systematically scaling such approaches, though our partial convergence  
524 scenarios may represent more realistic near-term targets given institutional constraints.

525 Scaling coordination mechanisms requires institutional frameworks aligned with existing  
526 governance structures. China's national carbon market, covering power and industrial sectors  
527 since 2021, provides such a platform.<sup>72</sup> Incorporating supply-chain emission credits would  
528 require mechanisms for allocating reductions between final producers and suppliers alongside  
529 verification protocols for upstream improvements. While detailed policy design remains for  
530 future development, the concentration of impacts offers practical entry points. With 3% of trade  
531 flows, primarily in the nonmetal, metal, and power sectors, accounting for 50% of emission  
532 burdens, targeted pilot programs could deliver substantial co-benefits before broader expansion.

533 Significant barriers remain despite these opportunities. Provincial governments often prioritize  
534 local GDP growth over cross-regional environmental objectives, while fragmented authority  
535 between environmental and economic agencies hampers coordination.<sup>73</sup> The absence of  
536 standardized mechanisms for cross-provincial technology transfer and benefit-sharing raises  
537 transaction costs, discouraging voluntary coordination.<sup>74,75</sup> These institutional constraints,  
538 combined with resource availability limitations, form key barriers to realizing identified co-  
539 benefits. Moreover, infrastructure lock-in embedded in existing energy and technological  
540 systems further constrains the pace and scope of energy intensity improvements.<sup>76</sup> Our

541 estimates, therefore, represent achievable benefits under reformed governance and gradual  
542 infrastructure adjustment, rather than outcomes expected under current institutional and  
543 technological arrangements.

544 Several limitations affect interpretation. First, the use of 2017 MRIO data does not capture  
545 recent supply chain restructuring under China's dual circulation strategy, likely underestimating  
546 current trade-embodied impacts. Second, VOC-related health impacts are not fully quantified.

547 This study adopts a combustion-based energy intensity framework. Electrification-related  
548 mitigation strategies, which offer more comprehensive co-mitigation prospects by  
549 simultaneously reducing CO<sub>2</sub> and VOC emissions, require fundamental restructuring of Input-  
550 Output relationships for accurate representation. Additionally, CMAQ v5.0 lacks several  
551 critical secondary organic aerosol formation pathways for VOCs, potentially underestimating  
552 their contribution to PM<sub>2.5</sub>-related health impacts.<sup>77</sup> Third, our convergence scenarios assume

553 static MRIO relationships, not accounting for how energy intensity improvements could  
554 reshape supply chain structures through price and substitution effects, alongside simplified  
555 treatment of technological and institutional path dependencies. Essential research directions

556 include dynamic modeling of final producer responses to carbon pricing to clarify policy  
557 effectiveness under different market conditions, sectoral analysis of coordination capacity  
558 variations to identify where final producer leverage is strongest, integration of electrification  
559 pathways into supply-chain co-mitigation frameworks, and assessment of how spatial  
560 redistribution of final production activities affects co-benefit distribution as China's industrial  
561 transformation continues. Extending this framework internationally could guide supply chain  
562 governance as climate policies expand globally, particularly for countries with pronounced

563 production-consumption separations.<sup>18,78</sup>

564

## 565 **ASSOCIATED CONTENT**

### 566 **Data Availability Statement**

567 Meteorological fields were generated using WRF v3.8.1 with grid nudging, driven by Global  
568 Forecast System (GFS) surface data from the National Centers for Environmental Prediction  
569 (NCEP), available at <https://www.nco.ncep.noaa.gov/pmb/products/gfs/#GFS>. The CMAQ  
570 Adjoint v5.0 model code can be accessed from the U.S. EPA GitHub repository  
571 ([https://github.com/USEPA/CMAQ\\_ADJOINT](https://github.com/USEPA/CMAQ_ADJOINT)) and its Zenodo archive  
572 (<https://zenodo.org/records/3780216>). The 2017 AiMa emission dataset used in this study can  
573 be accessed at <https://doi.org/10.5281/zenodo.17199169>. The Global Emission Modeling  
574 System (GEMS) inventory can be accessed at <https://gems.sustech.edu.cn/home>. The 2017  
575 Chinese Multi-regional Input-Output table is available from the CEADs database  
576 ([https://www.ceads.net/data/input\\_output\\_tables/](https://www.ceads.net/data/input_output_tables/)). Source attribution analysis was performed  
577 using MATLAB R2021a.

578 **Supporting Information.** Supplementary figures 1–15; supplementary tables 1–4;  
579 Supplementary texts 1–7, including methodological framework, emissions and health impacts  
580 embodied in the supply chains, GEMS inventory source information, MRIO sector  
581 classification, fitted parameters for IER model, model evaluation, health impact attribution  
582 analysis, mapping of GEMS emissions to the MRIO table, and uncertainty analysis.

## 583 **DECLARATION of COMPETING INTEREST**

584 The authors declare that they have no known competing financial interests or personal

585 relationships that could have appeared to influence the work reported in this paper.

## 586 **ACKNOWLEDGEMENT**

587 Y.C., H.S., and G.S. acknowledge funding from the Ministry of Science and Technology of the  
588 People's Republic of China (2023YFE0112900), Y.C. acknowledges funding from the National  
589 Natural Science Foundation of China (42571087), Y.C. and T.S. acknowledge funding from the  
590 National Natural Science Foundation of China (42330709), J.D. and H.S. acknowledge support  
591 from the Center for Computational Science and Engineering at Southern University of Science  
592 and Technology.

## 593 **AUTHOR CONTRIBUTIONS**

594 Y.C. conceived and supervised the study. J.D. and Y.C. processed and analyzed the data. H.S.,  
595 J.M.M., and S.T. contributed to the development of the model framework. D.J. and Y.C. drafted  
596 the manuscript. H.S., G.S., and S.T. participated in the result discussions. J.M., J.M.M., A.G.R.,  
597 S.Z., and A.H. provided critical revisions.

598

## 599 **REFERENCES**

- 600 (1) Cohen, A. J.; Brauer, M.; Burnett, R.; Anderson, H. R.; Frostad, J.; Estep, K.;  
601 Balakrishnan, K.; Brunekreef, B.; Dandona, L.; Dandona, R.; Feigin, V.; Freedman, G.;  
602 Hubbell, B.; Jobling, A.; Kan, H.; Knibbs, L.; Liu, Y.; Martin, R.; Morawska, L.; Pope,  
603 C. A.; Shin, H.; Straif, K.; Shaddick, G.; Thomas, M.; van Dingenen, R.; van Donkelaar,  
604 A.; Vos, T.; Murray, C. J. L.; Forouzanfar, M. H. Estimates and 25-year trends of the  
605 global burden of disease attributable to ambient air pollution: an analysis of data from  
606 the Global Burden of Diseases Study 2015. *Lancet* **2017**, *389* (10082), 1907–1918.
- 607 (2) National Development and Reform Commission (NDRC). *Enhanced Actions on climate  
608 change: China's Intended Nationally Determined Contributions*. 2015.  
609 [https://english.www.gov.cn/archive/publications/2015/07/01/content\\_281475138245408.htm](https://english.www.gov.cn/archive/publications/2015/07/01/content_281475138245408.htm) (accessed 2024-11-08).
- 611 (3) Yue, H.; He, C.; Huang, Q.; Yin, D.; Bryan, B. A. Stronger policy required to  
612 substantially reduce deaths from PM<sub>2.5</sub> pollution in China. *Nat. Commun.* **2020**, *11*, 1462.
- 613 (4) Shindell, D.; Smith, C. J. Climate and air-quality benefits of a realistic phase-out of

614 fossil fuels. *Nature* **2019**, *573*, 408–411.

615 (5) Wang, P.; Lin, C. K.; Wang, Y.; Liu, D.; Song, D.; Wu, T. Location-specific co-benefits  
616 of carbon emissions reduction from coal-fired power plants in China. *Nat. Commun.*  
617 **2021**, *12*, 6948.

618 (6) Geng, G.; Zheng, Y.; Zhang, Q.; Xue, T.; Zhao, H.; Tong, D.; Zheng, B.; Li, M.; Liu,  
619 F.; Hong, C.; He, K.; Davis, S. J. Drivers of PM<sub>2.5</sub> air pollution deaths in China 2002–  
620 2017. *Nat. Geosci.* **2021**, *14*, 645–650.

621 (7) Zhang, S.; An, K.; Li, J.; Weng, Y.; Zhang, S.; Wang, S.; Cai, W.; Wang, C.; Gong, P.  
622 Incorporating health co-benefits into technology pathways to achieve China's 2060  
623 carbon neutrality goal: a modelling Study. *Lancet Planet. Heal.* **2021**, *5* (11), e808–e817.

624 (8) Cheng, J.; Tong, D.; Liu, Y.; Geng, G.; Davis, S. J.; He, K.; Zhang, Q. A synergistic  
625 approach to air pollution control and carbon neutrality in China can avoid millions of  
626 premature deaths annually by 2060. *One Earth* **2023**, *6* (8), 978–989.

627 (9) Li, X.; Xu, H. The Energy-conservation and Emission-reduction Paths of Industrial  
628 Sectors: Evidence from Chinas 35 Industrial Sectors. *Energy Econ.* **2020**, *86*, 104628.

629 (10) Miller, S. A.; Moore, F. C. Climate and health damages from global concrete production.  
630 *Nat. Clim. Chang.* **2020**, *10*, 439–443.

631 (11) Chen, Y.; Shen, H.; Shen, G.; Ma, J.; Cheng, Y.; Russell, A. G.; Zhao, S.; Hakami, A.;  
632 Tao, S. Substantial differences in source contributions to carbon emissions and health  
633 damage necessitate balanced synergistic control plans in China. *Nat. Commun.* **2024**,  
634 *15*, 5880.

635 (12) Ma, T.; Zhang, S.; Xiao, Y.; Liu, X.; Wang, M.; Wu, K.; Shen, G.; Huang, C.; Fang, Y.  
636 R.; Xie, Y. Costs and health benefits of the rural energy transition to carbon neutrality  
637 in China. *Nat. Commun.* **2023**, *14*, 1601.

638 (13) Zhu, S.; Mac Kinnon, M.; Carlos-Carlos, A.; Davis, S. J.; Samuels, S.  
639 Decarbonization will lead to more equitable air quality in California. *Nat. Commun.*  
640 **2022**, *13*, 5738.

641 (14) Chen, C.; Sun, Y.; Lan, Q.; Jiang, F. Impacts of industrial agglomeration on pollution  
642 and ecological efficiency-A spatial econometric analysis based on a big panel dataset of  
643 China's 259 cities. *J. Clean. Prod.* **2020**, *258*, 120721.

644 (15) Wang, Y.; Wang, J. Does industrial agglomeration facilitate environmental performance:  
645 New evidence from urban China? *J. Environ. Manage.* **2019**, *248*, 109244.

646 (16) Li, X.; Xu, Y.; Yao, X. Effects of industrial agglomeration on haze pollution: A Chinese  
647 city-level study. *Energy Policy* **2021**, *148*, 111928.

648 (17) Lin, J.; Du, M.; Chen, L.; Feng, K.; Liu, Y.; Martin, R. V.; Wang, J.; Ni, R.; Zhao, Y.;  
649 Kong, H.; Weng, H.; Liu, M.; van Donkelaar, A.; Liu, Q.; Hubacek, K. Carbon and  
650 health implications of trade restrictions. *Nat. Commun.* **2019**, *10*, 4947.

651 (18) Nansai, K.; Tohno, S.; Chatani, S.; Kanemoto, K.; Kagawa, S.; Kondo, Y.; Takayanagi,  
652 W.; Lenzen, M. Consumption in the G20 nations causes particulate air pollution  
653 resulting in two million premature deaths annually. *Nat. Commun.* **2021**, *12*, 6286.

654 (19) Zheng, L.; Adalibieke, W.; Zhou, F.; He, P.; Chen, Y.; Guo, P.; He, J.; Zhang, Y.; Xu,  
655 P.; Wang, C.; Ye, J.; Zhu, L.; Shen, G.; Fu, T. M.; Yang, X.; Zhao, S.; Hakami, A.;  
656 Russell, A. G.; Tao, S.; Meng, J.; Shen, H. Health burden from food systems is highly  
657 unequal across income groups. *Nat. Food* **2024**, *5*, 251–261.

658 (20) Zhao, H.; Wu, R.; Liu, Y.; Cheng, J.; Geng, G.; Zheng, Y.; Tian, H.; He, K.; Zhang, Q.  
659 Air pollution health burden embodied in China's supply chains. *Environ. Sci.  
660 Ecotechnol.* **2023**, *16*, 100264.

661 (21) Malik, A.; Lenzen, M.; Li, M.; Mora, C.; Carter, S.; Giljum, S.; Lutter, S.; Gómez-  
662 Paredes, J. Polarizing and equalizing trends in international trade and Sustainable  
663 Development Goals. *Nat. Sustain.* **2024**, *7*, 1359–1370.

664 (22) Cao, C.; Cui, X. Q.; Cai, W.; Wang, C.; Xing, L.; Zhang, N.; Shen, S.; Bai, Y.; Deng,  
665 Z. Incorporating health co-benefits into regional carbon emission reduction policy  
666 making: A case study of China's power sector. *Appl. Energy* **2019**, *253*, 113498.

667 (23) Tang, R.; Zhao, J.; Liu, Y.; Huang, X.; Zhang, Y.; Zhou, D.; Ding, A.; Nielsen, C. P.;  
668 Wang, H. Air quality and health co-benefits of China's carbon dioxide emissions  
669 peaking before 2030. *Nat. Commun.* **2022**, *13*, 1008.

670 (24) Xia, C.; Zheng, H.; Meng, J.; Shan, Y.; Liang, X.; Li, J.; Yin, Z.; Chen, M.; Du, P.;  
671 Wang, C. Outsourced carbon mitigation efforts of Chinese cities from 2012 to 2017.  
672 *Nat. Cities* **2024**, *1*, 480–488.

673 (25) Zhang, H.; Zhang, W.; Lu, Y.; Wang, Y.; Shan, Y.; Ping, L.; Li, H.; Lee, L. C.; Wang,  
674 T.; Liang, C.; Jiang, H.; Cao, D. Worsening Carbon Inequality Embodied in Trade  
675 within China. *Environ. Sci. Technol.* **2023**, *57* (2), 863–873.

676 (26) He, K.; Mi, Z.; Zhang, J.; Li, J.; Coffman, D. The Polarizing Trend of Regional CO<sub>2</sub>  
677 Emissions in China and Its Implications. *Environ. Sci. Technol.* **2023**, *57* (11), 4406–  
678 4414.

679 (27) Zhang, W.; Zhao, J.; Zhang, Z.; Liu, M.; Li, R.; Xue, W.; Xing, J.; Cai, B.; Jiang, L.;  
680 Zhang, J.; Hu, X.; Zhong, L.; Jiang, H.; Wang, J.; Bi, J. The economy–employment–  
681 environmental health transfer and embedded inequities of China's capital metropolitan  
682 area: a mixed-methods study. *Lancet Planetary Health* **2023**, *7*, e912–e924.

683 (28) Wang, H.; Zhang, Y.; Zhao, H.; Lu, X.; Zhang, Y.; Zhu, W.; Nielsen, C. P.; Li, X.; Zhang,  
684 Q.; Bi, J.; McElroy, M. B. Trade-driven relocation of air pollution and health impacts in  
685 China. *Nat. Commun.* **2017**, *8*, 738.

686 (29) Zhao, H.; Li, X.; Zhang, Q.; Jiang, X.; Lin, J.; Peters, G. P.; Li, M.; Geng, G.; Zheng,  
687 B.; Huo, H.; Zhang, L.; Wang, H.; Davis, S. J.; He, K. Effects of atmospheric transport  
688 and trade on air pollution mortality in China. *Atmos. Chem. Phys.* **2017**, *17*, 10367–  
689 10381.

690 (30) Hakami, A.; Henze, D. K.; Seinfeld, J. H.; Singh, K.; Sandu, A.; Kim, S.; Byun, D.; Li,  
691 Q. The Adjoint of CMAQ. *Environ. Sci. Technol.* **2007**, *41* (22), 7807–7817.

692 (31) Zhao, S.; Russell, M. G.; Hakami, A.; Capps, S. L.; Turner, M. D.; Henze, D. K.; Percell,  
693 P. B.; Resler, J.; Shen, H.; Russell, A. G.; Nenes, A.; Pappin, A. J.; Napelenok, S. L.;  
694 Bash, J. O.; Fahey, K. M.; Carmichael, G. R.; Stanier, C. O.; Chai, T. A multiphase  
695 CMAQ version 5.0 adjoint. *Geosci. Model Dev.* **2020**, *13* (7), 2925–2944.

696 (32) Byun, D.; Schere, K. L. Review of the Governing Equations, Computational Algorithms,  
697 and Other Components of the Models-3 Community Multiscale Air Quality (CMAQ)  
698 Modeling System. *Appl. Mech. Rev.* **2006**, *59*, 51–77.

699 (33) Henze, D. K.; Seinfeld, J. H.; Shindell, D. T. Inverse modeling and mapping US air  
700 quality influences of inorganic PM<sub>2.5</sub> precursor emissions using the adjoint of GEOS-  
701 Chem. *Atmos. Chem. Phys.* **2009**, *9*, 5877–5903.

702 (34) Zhao, H.; Geng, G.; Zhang, Q.; Davis, S. J.; Li, X.; Liu, Y.; Peng, L.; Li, M.; Zheng, B.;  
703 Huo, H.; Zhang, L.; Henze, D. K.; Mi, Z.; Liu, Z.; Guan, D.; He, K. Inequality of  
704 household consumption and air pollution-related deaths in China. *Nat. Commun.* **2019**,  
705 *10*, 4337.

706 (35) Wang, Y.; Bastien, L.; Jin, L.; Harley, R. A. Location-Specific Control of Precursor  
707 Emissions to Mitigate Photochemical Air Pollution. *Environ. Sci. Technol.* **2023**, *57*  
708 (26), 9693–9701.

709 (36) AiMa Forecasts. AiMa Air Quality Forecasting System. <http://www.aimayubao.com>  
710 (accessed 2021-01-17)

711 (37) Lyu, B.; Zhang, Y.; Hu, Y. Improving PM<sub>2.5</sub> Air Quality Model Forecasts in China  
712 Using a Bias-Correction Framework. *Atmosphere* **2017**, *8* (8), 147.

713 (38) Lyu, B.; Hu, Y.; Zhang, W.; Du, Y.; Luo, B.; Sun, X.; Sun, Z.; Deng, Z.; Wang, X.; Liu,  
714 J.; Wang, X.; Russell, A. G. Fusion Method Combining Ground-Level Observations  
715 with Chemical Transport Model Predictions Using an Ensemble Deep Learning  
716 Framework: Application in China to Estimate Spatiotemporally-Resolved PM<sub>2.5</sub>  
717 Exposure Fields in 2014–2017. *Environ. Sci. Technol.* **2019**, *53* (13), 7306–7315.

718 (39) Shen, H.; Shen, G.; Chen, Y.; Russell, A. G.; Hu, Y.; Duan, X.; Meng, W.; Xu, Y.; Yun,  
719 X.; Lyu, B.; Zhao, S.; Hakami, A.; Guo, J.; Tao, S.; Smith, K. R. Increased air pollution  
720 exposure among the Chinese population during the national quarantine in 2020. *Nat.  
721 Hum. Behav.* **2021**, *5*, 239–246.

722 (40) Shen, H.; Sun, Z.; Chen, Y.; Russell, A. G.; Hu, Y.; Odman, M. T.; Qian, Y.; Archibald,  
723 A. T.; Tao, S. Novel Method for Ozone Isopleth Construction and Diagnosis for the  
724 Ozone Control Strategy of Chinese Cities. *Environ. Sci. Technol.* **2021**, *55* (23),  
725 15625–15636.

726 (41) Skamarock, W. C.; Klemp, J. B.; Dudhia, J.; Gill, D. O.; Barker, D. M.; Duda, M. G.;  
727 Huang, X. Y.; Wang, W.; Powers, J. G. *A Description of the Advanced Research WRF  
728 Version 3*; NCAR Tech Notes-475+STR, National Center for Atmospheric Research  
729 (NCAR), 2008.

730 (42) National Centers for Environmental Prediction (NCEP). NCEP Products Inventory:  
731 Global Products, Global Forecast System (GFS) Model;  
732 <https://www.nco.ncep.noaa.gov/pmb/products/gfs/#GFS> (accessed 2021-01-17).

733 (43) Emery, C.; Liu, Z.; Russell, A.G.; Odman, M.T.; Yarwood, G.; Kumar, N.  
734 Recommendations on statistics and benchmarks to assess photochemical model  
735 performance. *J. Air Waste Manag. Assoc.* **2017**, *67* (5), 582–598.

736 (44) Zhai, H.; Huang, L.; Emery, C.; Zhang, X.; Wang, Y.; Yarwood, G.; Fu, J. S.; Li, L.  
737 Recommendations on benchmarks for photochemical air quality model applications in  
738 China—NO<sub>2</sub>, SO<sub>2</sub>, CO and PM<sub>10</sub>. *Atmos. Environ.* **2024**, *319*, 120290.

739 (45) GEMS. Global Emission Modeling System (GEMS): A comprehensive global emission  
740 inventory for greenhouse gases and air pollutants. <https://gems.sustech.edu.cn/home>  
741 (accessed 2024-06-17).

742 (46) Huang, Y.; Shen, H.; Chen, H.; Wang, R.; Zhang, Y.; Su, S.; Chen, Y.; Lin, N.; Zhuo, S.;  
743 Zhong, Q.; Wang, X.; Liu, J.; Li, B.; Liu, W.; Tao, S. Quantification of Global Primary  
744 Emissions of PM<sub>2.5</sub>, PM<sub>10</sub>, and TSP from Combustion and Industrial Process Sources.  
745 *Environ. Sci. Technol.* **2014**, *48* (23), 13834–13843.

746 (47) Peters, G. P. From production-based to consumption-based national emission  
747 inventories. *Ecol. Econ.* **2008**, *65* (1), 13–23.

748 (48) Liang, S.; Zhang, C.; Wang, Y.; Xu, M.; Liu, W. Virtual Atmospheric Mercury  
749 Emission Network in China. *Environ. Sci. Technol.* **2014**, *48* (5), 2807–2815.

750 (49) Li, R.; Zhang, J.; Krebs, P. Global trade drives transboundary transfer of the health  
751 impacts of polycyclic aromatic hydrocarbon emissions. *Commun. Earth Environ.* **2022**,  
752 3, 170.

753 (50) Zheng, H.; Bai, Y.; Wei, W.; Meng, J.; Zhang, Z.; Song, M.; Guan, D. Chinese  
754 provincial multi-regional input-output database for 2012, 2015, and 2017. *Sci. Data*  
755 **2021**, *8*, 244.

756 (51) National Bureau of Statistics. China Statistical Yearbook 2018. China Statistics Press:  
757 Beijing, 2019.

758 (52) National Bureau of Statistics. China Energy Statistical Yearbook 2018. China Statistics  
759 Press: Beijing, 2019.

760 (53) Tang, L.; Qu, J.; Mi, Z.; Bo, X.; Chang, X.; Anadon, L. D.; Wang, S.; Xue, X.; Li, S.;  
761 Wang, X.; Zhao, X. Substantial emission reductions from Chinese power plants after  
762 the introduction of ultra-low emissions standards. *Nat. Energy* **2019**, *4*, 929–938.

763 (54) Feng, K.; Davis, S. J.; Sun, L.; Li, X.; Guan, D.; Liu, W.; Liu, Z.; Hubacek, K.  
764 Outsourcing CO<sub>2</sub> within China. *Proc. Natl. Acad. Sci. U. S. A.* **2013**, *110* (28), 11654–  
765 11659.

766 (55) Shen, J.; Wei, Y. D.; Yang, Z. The impact of environmental regulations on the location  
767 of pollution-intensive industries in China. *J. Clean. Prod.* **2017**, *148*, 785–794.

768 (56) Wu, W.; Tang, Q.; Xue, W.; Shi, X.; Zhao, D.; Liu, Z.; Liu, X.; Jiang, C.; Yan, G.;  
769 Wang, J. Quantifying China's iron and steel industry's CO<sub>2</sub> emissions and  
770 environmental health burdens: A pathway to sustainable transformation. *Environ. Sci.  
771 Ecotechnol.* **2024**, *20*, 100367.

772 (57) Shu, Z.; Zhao, T.; Liu, Y.; Zhang, L.; Ma, X.; Kuang, X.; Li, Y.; Huo, Z.; Ding, Q.; Sun,  
773 X.; Shen, L. Impact of deep basin terrain on PM<sub>2.5</sub> distribution and its seasonality over  
774 the Sichuan Basin, Southwest China. *Environ. Pollut.* **2022**, *300*, 118944.

775 (58) Zeng, P.; Zong, C. Research on the relationship between population distribution pattern  
776 and urban industrial facility agglomeration in China. *Sci. Rep.* **2023**, *13*, 16225.

777 (59) Sun, X.; Li, J.; Qiao, H.; Zhang, B. Energy implications of China's regional  
778 development: New insights from multi-regional input-output analysis. *Appl. Energy*  
779 **2017**, *196*, 118–131.

780 (60) Shao, S.; Wang, C.; Guo, Y.; Yang, L.; Chen, S.; Yan, J.; Shan, Y.; Liu, Z.; Guan, D.  
781 Enlarging Regional Disparities in Energy Intensity within China. *Earth's Future* **2020**,  
782 8 (8), e2020EF001572.

783 (61) Jiao, J.; Chen, C.; Bai, Y. Is green technology vertical spillovers more significant in  
784 mitigating carbon intensity? Evidence from Chinese industries. *J. Clean. Prod.* **2020**,  
785 257, 120354.

786 (62) Tong, B.; Zhang, L.; Hou, Y.; Oenema, O.; Long, W.; Velthof, G.; Ma, W.; Zhang, F.  
787 Lower pork consumption and technological change in feed production can reduce the  
788 pork supply chain environmental footprint in China. *Nat. Food* **2023**, *4*, 74–83.

789 (63) Rahko, J. Vertical spillovers and the energy intensity of European industries. *Energy*

790 *Econ.* **2025**, *141*, 108053.

791 (64) Apple Inc. *Supplier Clean Energy Program Update 2022*.  
[https://www.apple.com/environment/pdf/Apple\\_Supplier\\_Clean\\_Energy\\_Program\\_Update\\_2022.pdf](https://www.apple.com/environment/pdf/Apple_Supplier_Clean_Energy_Program_Update_2022.pdf) (accessed 2025-09-28).

792 (65) Liu, D. *Clean Development Mechanism (CDM)*. In *The Palgrave Encyclopedia of Global Security Studies*; Romaniuk, S. N.; Marton, P. N., Eds.; Palgrave Macmillan: Cham. 2023.

793 (66) Wang, E. -Z.; Pan, T. Does ISO 50001 adoption reduce manufacturing energy intensity? Micro-evidence from China. *Econ. Anal. Policy* **2025**, *86*, 653–672.

794 (67) Pimm, A. J.; Cockerill, T. T.; Gale, W. F. Energy system requirements of fossil-free steelmaking using hydrogen direct reduction. *J. Clean. Prod.* **2021**, *312*, 127665.

795 (68) Asian Development Bank. *Policies and Investments to Address Climate Change and Air Quality in Beijing-Tianjin-Hebei Region*.  
[https://www.adb.org/sites/default/files/publication/844441/climate-change-air-quality-beijing-tianjin-hebei\\_0.pdf](https://www.adb.org/sites/default/files/publication/844441/climate-change-air-quality-beijing-tianjin-hebei_0.pdf) (accessed 2025-09-28).

796 (69) Du, H.; Zhao, L.; Zhang, P.; Li, J.; Yu, S. Ecological compensation in the Beijing-Tianjin-Hebei region based on ecosystem services flow. *J. Environ. Manage.* **2023**, *331*, 117230.

797 (70) National People's Congress. *Beijing, Tianjin, Hebei to come closer for development, according to local legislature*. [http://en.npc.gov.cn/cdurl.cn/2024-02/08/c\\_962573.htm](http://en.npc.gov.cn/cdurl.cn/2024-02/08/c_962573.htm) (accessed 2025-09-28).

798 (71) The State Council of the People's Republic of China. *Major steel province makes headway in eco-friendly growth*.  
[https://english.www.gov.cn/news/topnews/202209/14/content\\_WS63212ae5c6d0a757729dff63.html](https://english.www.gov.cn/news/topnews/202209/14/content_WS63212ae5c6d0a757729dff63.html) (accessed 2025-09-28).

799 (72) Ministry of Ecology and Environment of the People's Republic of China. *Work Plan for Including Steel, Cement, and Aluminum Smelting Industries in the National Carbon Emissions Trading Market*.  
[https://www.mee.gov.cn/xxgk2018/xxgk/xxgk03/202503/t20250326\\_1104736.html](https://www.mee.gov.cn/xxgk2018/xxgk/xxgk03/202503/t20250326_1104736.html) (accessed 2025-03-28).

800 (73) Qi, Y.; Zhang, L. Local Environmental Enforcement Constrained by Central–Local Relations in China. *Environ. Policy Gov.* **2014**, *24* (3), 216–232.

801 (74) Banerjee, S.; Cason, T. N.; de Vries, F. P.; Hanley, N. Transaction costs, communication and spatial coordination in Payment for Ecosystem Services Schemes. *J. Environ. Econ. Manage.* **2017**, *83*, 68–89.

802 (75) Sun, Y.; Grimes, S. The actors and relations in evolving networks: The determinants of inter-regional technology transaction in China. *Technol. Forecast. Soc. Change* **2017**, *125*, 125–136.

803 (76) Seto, K. C.; Davis, S. J.; Mitchell, R. B.; Stokes, E. C.; Unruh, G.; Ürge-Vorsatz, D. Carbon Lock-In: Types, Causes, and Policy Implications. *Annu. Rev. Environ. Resour.* **2016**, *41*, 425–452.

804 (77) Wu, R.; Tessum, C. W.; Zhang, Y.; Hong, C.; Zheng, Y.; Qin, X.; Liu, S.; Zhang, Q. Reduced-complexity air quality intervention modeling over China: the development of InMAPv1.6.1-China and a comparison with CMAQv5.2. *Geosci. Model Dev.* **2021**, *14*

834 (12), 7621–7638.

835 (78) Wang, Z.; Meng, J.; Zheng, H.; Shao, S.; Wang, D.; Mi, Z.; Guan, D. Temporal change  
836 in India's imbalance of carbon emissions embodied in international trade. *Appl. Energy*  
837 **2018**, *231*, 914–925.